Advances in Science and Technology Research Journal

Advances in Science and Technology Research Journal 2024, 18(3), 33–44
https://doi.org/10.12913/22998624/185505
ISSN 2299-8624, License CC-BY 4.0

Received: 2023.12.30
Accepted: 2024.02.28
Published: 2024.04.20

Effect of Trenched Hemispherical Pin Fins on Cooling Performance of Heat Sink

Aissa Yousfi[1], Lahcene Bellahcene[2], Faris Alqurashi[3], Djamel Sahel[4], Mohamed Teggar[2], Abdelghani Laouer[5], Müslüm Arici[6], Mohamed Kchaou[3*]

[1] LEDMSD, University Amar Telidji, Laghouat 03000, Algeria
[2] LMe, University Amar Telidji, Laghouat 03000, Algeria
[3] Department of Mechanical Engineering, College of Engineering, University of Bisha, P.O. Box 001, Bisha, Saudi Arabia
[4] LCGE Laboratory, UST-Oran-MB, Oran 31000, Algeria
[5] LPMCN Laboratory, Faculty of Exact Sciences and Computer Science, University of Jijel, 18000, Jijel, Algeria
[6] Mechanical Engineering Department, Engineering Faculty, Kocaeli University, Turkey
* Corresponding author's e-mail: kchaou.mohamed@yahoo.fr

ABSTRACT

Pin fins have the potential to improve the thermal performance of various engineering devices. Modified pin fins could further increase their thermal performance in a passive way at lower cost. This study is aimed at numerically investigating the thermal performance of trenched hemispherical pin fins heat sink (THPFHS) and the influence of parameters including the trench number (N = 1, 3 and 5) and thickness (e = 1 to 5 mm). The simulations were performed using a computational fluid dynamics (CFD) software considering turbulent air flow conditions. Results showed that the use of aluminum fins fitted with one trench in the middle of the hemispherical pin fin considerably increased the local heat transfer. Furthermore, all studied configurations show high thermal performance factor (HTPF) compared with the conventional cylindrical pin fins heat sink (CPFHS). For this new configuration (THPFHS), Nu increases by 45% while the thermal resistance reduces by 42%, compared to the baseline case. On the other hand, this improved performance results in 50% pressure drop penalty. Moreover, the obtained results showed a significant improvement in the performance mainly at high Re.

Keywords: cooling; heat sink, trench, hemispherical, pin fin, performance analysis.

INTRODUCTION

Nowadays, the immense development of computer technologies has risen to the challenge for cooling electronic devices. Further, downsized heat sink decreases the heat exchange surface area. Under these undesirable conditions, heat flux evacuated by the electronic components causes overheat and threatens the functionality of these systems. Researchers are addressing this challenge and investigating solutions [1, 2]. Thus, pin fins heat sinks (PFHS) are gaining attention of investigators. Meinders et al. [3] studied the flow behavior behind pins and showed its significance for heat transfer and thermal management. Another research group [4] numerically addressed the potential of perforated-PFHS for thermal performance improvement. They highlighted the impact of geometrical parameters. An investigation was performed on a new pin fin shape (pyramid) [5], this shape had an improving effect on the performance of heat sinks, as concluded by the authors. Another numerical study

[6] was devoted to thermal-hydraulic performance of perforated-PFHS which showed higher performance than solid-PFHS. Ismail et al. [7] investigated various perforated-PFHS; they proposed holes in square, circular, triangular and hexagonal shapes. Compared with the other arrangements, perforated-PFHS with circular holes showed the best thermal performance. In this regard, it was confirmed that the perforated pin fin is one of successful techniques for thermal management [8, 9]. Reid and collaborators [10] addressed the design optimization of passive heat sinks by using SIMULIA-Tosca and SIMULIA-Abaqus. The topology optimization method generated in the study was obtained by varying manufacturing and volume constraints. They reported that the best design resulted in lower peak temperature estimated by 24%. Huang et al. [11] investigated optimization of the pin hole size of perforated-PFHS aiming to minimize both ΔT and Δp. Shi Zeng et al. [12] numerically studied two types of fin configurations for liquid-cooled micro-channel heat sinks. They showed that the proposed new fin pattern thermally outperforms the other investigated designs. Sahel et al. [13] reported also similar findings of the high thermal performance of perforated-PFHS. Pan et al. [14] proposed a staggered pin fin configuration which can considerably improve the heat dissipation rate in heat sinks. In this context, the configuration and size of the pins were able to reduce the recirculation zones and hot spots behind the pins [15, 16] and consequently increased the heat transfer coefficients in the cooling system.

Hybrid nanofluids, which are based on additives of both types i.e. metallics and non-metallics, have gained attention in recent years due to their potential use in heat dissipation applications, particularly in heat sink systems. Heiarshenas et al. [17] showed that using the novel hybrid nanofluid composed of ionic liquid-alumina nanoparticles in a water-based solution can greatly improve the thermal performance of heat sinks. Nanoparticles of 20 and 50 nm resulted in 26% higher thermal performance than that shown in the case of pure water, resulting hence in a significant increase in the heat dissipation rate. Kumar et al. [18] investigated the use of a hybrid nanofluid composed of grapheme and Platinum nanoparticles suspended in water for heat dissipation in electronics devices. Addition of grapheme nanoparticles significantly increased the thermal conductivity of the cooling fluid. Hybrid nanofluid could potentially lead to more efficient heat dissipation rate in electronic devices. Sriharan et al. [19] experimentally investigated the impact of nanoparticles of hybrid water nanofluid. Higher performance and heat transfer enhancement of up to 54% were obtained with nanofluids, compared to the pure water performance.

The configuration of pin fins plays a key role in the heat sink design and thermal performance. Thus, intensive research investigated this type of heat transfer enhancement [20, 21]. Khetib et al. [22] numerically investigated this enhancing effect, three-pin configurations were investigated alongside their geometrical parameters. A similar study was conducted by Nilpueng et al. [23] where the impact of fin pitch was emphasized. Yakut et al. [24] employed an optimization method for design of efficient fins. They found out the optimal size for hexagon-shaped pin fins. Recently, phase change materials (PCMs) have been one of the most investigated passive methods for thermal management. Several works have been conducted to enhance the passive cooling of pin fins heat sink using PCMs [25-27]. Arshad et al. [28] experimentally studied cooling of electronics. Paraffin wax and aluminum square fins were investigated for fin thicknesses varying from 1 mm to 3 mm for various heat fluxes. It was found that the optimal performance in terms of operating time is achieved for 2 mm of fin thickness. Ali et al. [29] experimentally analyzed three different configurations of PFHS using various PCMs. Triangular fins were found to be the most efficient fin design.

The present study is aimed at improving the thermal performance of a hemispherical pin fins heat sink (HSPFHS) by considering trenches in the hemispherical heat sinks. The influence of the number (1, 3, and 5) and trench thickness (from 1 mm to 5 mm) on the thermo-hydraulic characteristics was examined through seven different configurations. The thermal performance and the fluid flow dynamics were examined. Nusselt number as well as pressure drop were analyzed as function of Reynolds number. The mass reduction was emphasized since the cost can be reduced while increasing the thermal performance.

MODELING

Configuration

The problem investigated in this paper is illustrated in Figure 1 consisting of a heat sink with hemispherical pin fins of radius R = 12 mm (Fig.

2) placed on a plate 100×100 mm. This heat sink is located inside an airflow channel of dimensions 240×100×12 mm. The staggered arranged HSPFs are shown in Figure 1, where the longitudinal spacing is S_L = 12.5 mm, and transversal spacing is S_T = 25 mm. Several cases were studied by varying the number and thickness of the trench (e = 1 mm, 2 mm, 3 mm, 4 mm, 5 mm). A5083P aluminum was used for both plate and fins (Table 1). Using hemispherical pin fins (HSPF) not only augments the thermal performance but also it helps reduce the occupied volume and mass of heat sinks [13]. Using the trenching technique in the HSPF is aimed for reduction of the hot points behind the pins.

Governing equations

Conservation equations governing heat transfer and fluid flow are used with assuming steady turbulent regime [30, 31], and incompressible flow. The RNG *k*-epsilon model of turbulence is used in this study because it is largely utilized to predict the turbulent flow and heat transfer inside pin fins heat sinks. It is based on the turbulent kinetic energy k (Eq. 6) and the energy dissipations ε (Eq. 5). In the case of steady-state conditions, the governing equations are:

Continuity equation:

$$\frac{\partial u_i}{\partial x_i} = 0 \tag{1}$$

Momentum equation:

$$\frac{\partial \left(u_i u_j\right)}{\partial x_j} = -\frac{\partial \overline{p}}{\partial x_i} + \nu \nabla^2 u_i + \frac{\partial}{\partial x_j}\left(-\overline{u_i' u_j'}\right) \tag{2}$$

Energy equation:

$$\frac{\partial \left(u_j T\right)}{\partial x_j} = \alpha \nabla^2 T + \frac{\partial}{\partial x_j}\left(-\overline{u_i' \theta}\right) \tag{3}$$

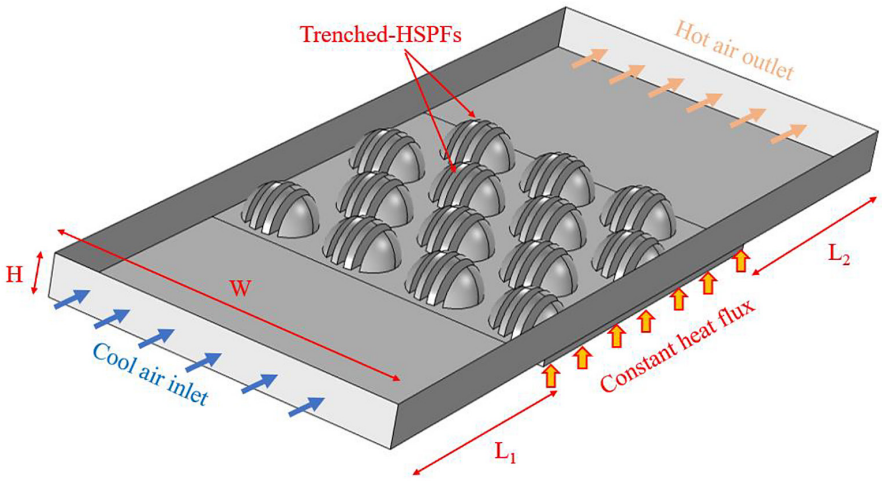

Fig. 1. Sketch of the trenched hemispherical pin fins heat sink

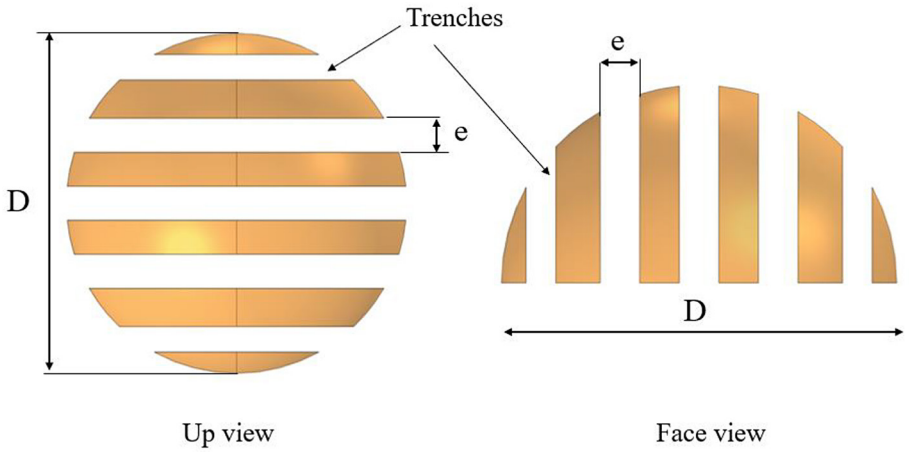

Fig. 2. Example of a pin with 5 trenches

Table 1. Material proprieties [30]

Parameter	Density (kg/m^3)	Thermal expansion (1/K)	Conductivity (W/m. K)
Values	2650	23.8	167

Heat conduction equation:

$$\nabla \cdot \left(\lambda_s \nabla T_s\right) = 0 \tag{4}$$

$$\rho(u.\nabla)\varepsilon = \nabla.\left[\left(\mu + \frac{\mu T}{\sigma\varepsilon}\right)\nabla\varepsilon\right] + C_{sl}\frac{\varepsilon}{k}P_k - C_{cl}\rho\frac{\varepsilon^2}{k} \tag{5}$$

$$\rho(u.\nabla)k = \nabla.\left[\left(\mu + \frac{\mu T}{\sigma k}\right)\nabla k\right] + P_k - \rho\varepsilon \tag{6}$$

$$P_k = \mu_T\left[\nabla u.\left(\nabla u + (\nabla u)^T\right)\right] \tag{7}$$

$$\mu_T = \rho C_\mu \frac{k^2}{\varepsilon} \tag{8}$$

$$\nabla p = p_{in} - p_{out} \tag{9}$$

where: p_{in} and p_{out} stand for pressures while the thermal resistance is:

$$R_{th} = \left(T_w - T_{in}\right)/q'' \tag{10}$$

$$\mathrm{Re} = \frac{UD_h}{v} \tag{11}$$

where: the D_h formula is written as follows:

$$D_h = \frac{4A_c}{P} \tag{12}$$

$$Nu = \frac{q'' D_h}{\lambda_{air}\left(T_w - \left(T_{in} + T_{out}\right)/2\right)} \tag{13}$$

The performance parameter is given by:

$$HTPF = \frac{\left(Nu/Nu_{CPFS}\right)}{\left(\Delta p/\Delta p_{CPFS}\right)^{1/3}} \tag{14}$$

RESULTS

Validation

Simulation was based on COMSOL Multiphysics® v. 5.4 software [32]. A numerical check was first performed to examine the mesh independency on the accuracy and reliability of numerical results. The structure and size of mesh (Fig. 3) were scrutinized regarding their crucial impact on the numerical results. To this end, tetrahedral meshes with various numbers of elements were generated and the resulting average Nusselt numbers were compared. To evaluate the grid convergence, cylindrical pin fins (CPFs) were analyzed at Re = 12820. Convergence was set to residuals less than 10^{-6}. Several grids were employed: 608112, 1100289, 1538157, 1822298, and 2102516 elements. Notably, Nu exhibited minimal variation (less than 1%) for the grids with a greater number of elements than 1538157, confirming their reliability as shown in Figure 4. As a result, the grid with 1538157 elements was chosen for the ultimate CPFs simulations. A similar approach of grid independency was applied to all configurations. Figure 3 illustrates the mesh structures.

After grid independency analysis, cylindrical pin fin heat sink (CPFHS) was validated by comparison with experimental and numerical data [30]. Figure 5a clearly demonstrates that the conducted numerical simulation effectively predicts the Nu variation with deviation less than 14%. This discrepancy can be attributed to the thermocouples used for temperature measurement (three at the inlet and three at the

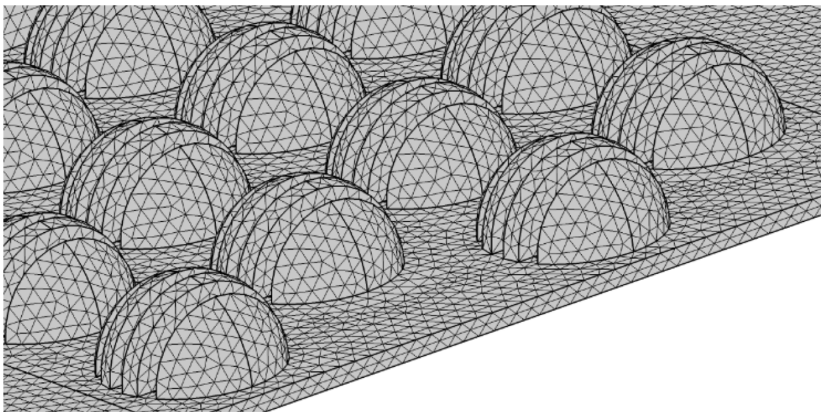

Fig. 3. Mesh grid of the heat sink

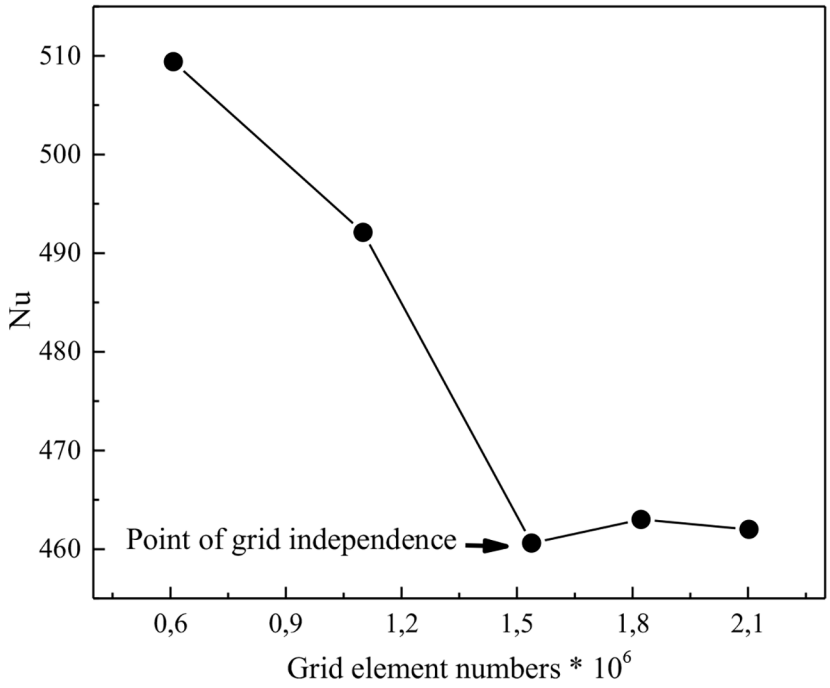

Fig. 4. Test of grid independency

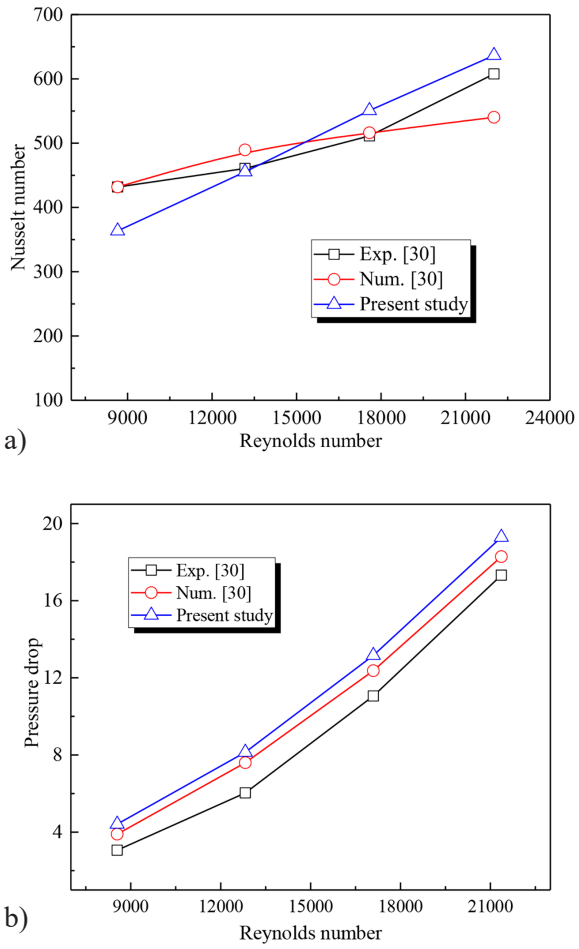

Fig. 5. Validation of results on CPFHs, for (a) Nusselt number and (b) pressure drop

outlet) compared with the adopted numerical model which is based on average temperatures. Additionally, Figure 5b shows the pressure drop validation with [30]. Deviations of 5% and 10% were obtained with the numerical and experimental data, respectively. Obviously, there is a good accordance of the results.

Effect of the trench thickness

Improvement of the performance of the hemispherical heat sink pin fins was investigated by creating trenches in the solid fins. Nu, thermal resistance (R_{th}), and pressure drop are examined for trench thickness (e) varying from 1 to 5 mm. Figs. 6 to 9 depict the variations of Nu, Δp, R_{th}, and the hydrothermal performance factor (HTPF) for different trench configurations and Re values. The impact of the trench thickness on Nu and Re is depicted in Figure 6. As it is shown, an optimal configuration (e = 1 mm) exhibits up to 45% enhancement in Nu indicating an improvement of heat dissipation, which can ensure a significant cooling effect for the electronic components.

Figures. 7, 8 show the pressure difference and thermal resistance (R_{th}), respectively, for a range of Reynolds numbers. The hemispherical pins in the case of trench thickness e = 1 mm lead to an increase in the pressure drop (Δp) up to 50%, this augmentation helps to block the air flow which improves the thermal performance. On the other hand,

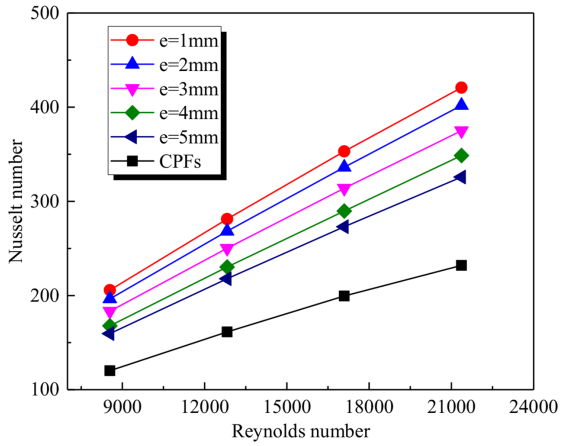

Fig. 6. Nusselt number vs Re

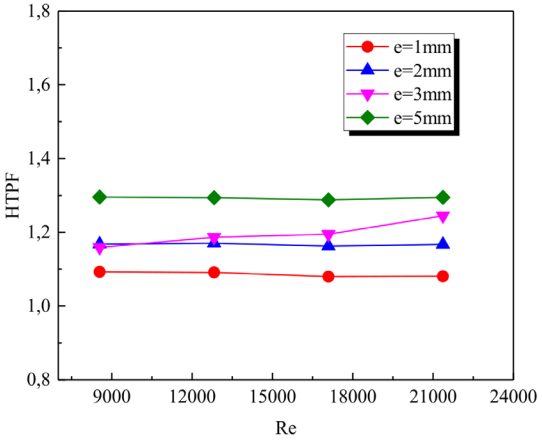

Fig. 9. Heat transfer performance criteria HTPF vs *Re*

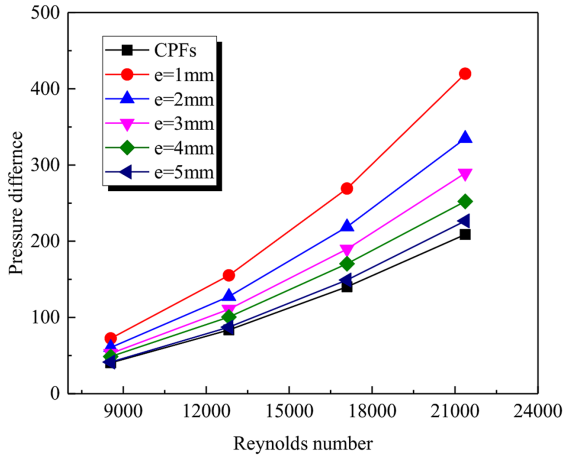

Fig. 7. Pressure difference (*Δp*) vs *Re*

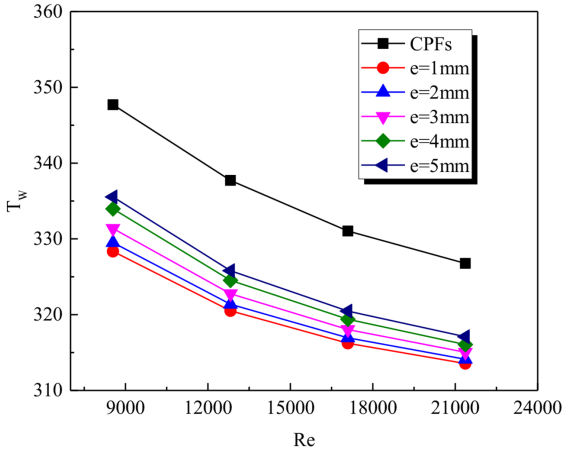

Fig. 10. Wall temperature vs *Re*

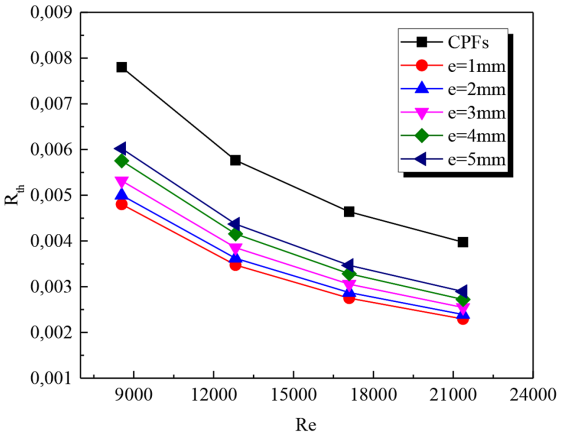

Fig. 8. Thermal resistance vs *Re*

the decrease in R_{th} by 42% in the case of e = 1 mm results in a temperature decrement. Simulations of the different cases are performed by using the same boundary conditions. Figure 9 shows 30% increase in the HTPF while Figure 10 illustrates the wall temperature variation with Reynolds number for hemispherical pin fins heat sink having different trench thickness. T_w decrement is due to augmentation of the turbulent intensity and inertial shears near the heat sink wall. Likewise, the decreases of the trench thickness contribute to reducing the wall temperature. Additionally, Figures 11 and 12 display the temperature distribution for e = 1, 2, 3, 4, 5 mm at Re = 21367. Obviously, lower temperature in the lower part of the cooling system is observed which increases with the size of trenches. For this reason, the hemispherical pin fin has been proposed to reduce the volume of the air-cooling channel and greatly increase the contact area near the heat source. The flow structure generally influences the heat transfer performance in heat sinks. As illustrated in Figure 12, the effect of trench thickness by the different flow structures can clearly be noticed. Decreasing recirculations are observed behind the pin fins with increasing the trench thickness.

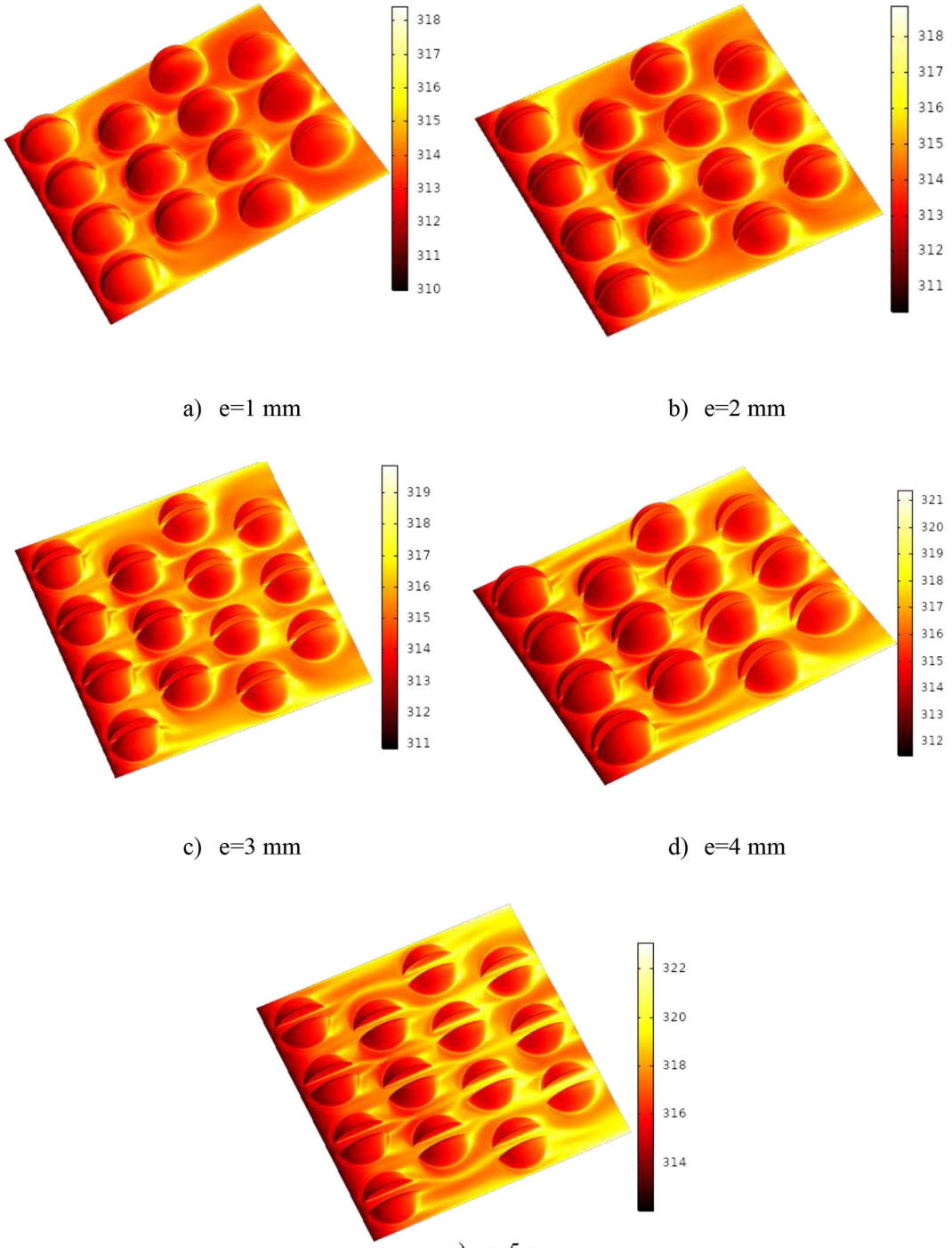

Fig. 11. Temperatures on the surface contact for e=1, 2, 3, 4, 5 mm and *Re* = 21367

Effect of the trenches number

This section was focused on the optimization of the configuration identified in the previous section. Different numbers of trenches are considered in the hemispherical pin fins heat sink. Figures 13. to 16 illustrate the variation of *Nu*, Δp, R_{th} and *HTPF* versus *Re* for hemispherical pin fins heat sinks having 3 and 5 trenches, respectively. According to Figure 13, *Nu* increases by 131% and 144% for three and five trenches, respectively. These augmentations demonstrate that increasing the trench number augments the heat transfer surface areas leading to higher cooling performance. Variation of the pressure drops (Δp) with Re is shown in Figure 14, for HSPFHS having 3 and 5 trenches. Increasing of *Re* increases Δp due to augmentation of the blockage. At

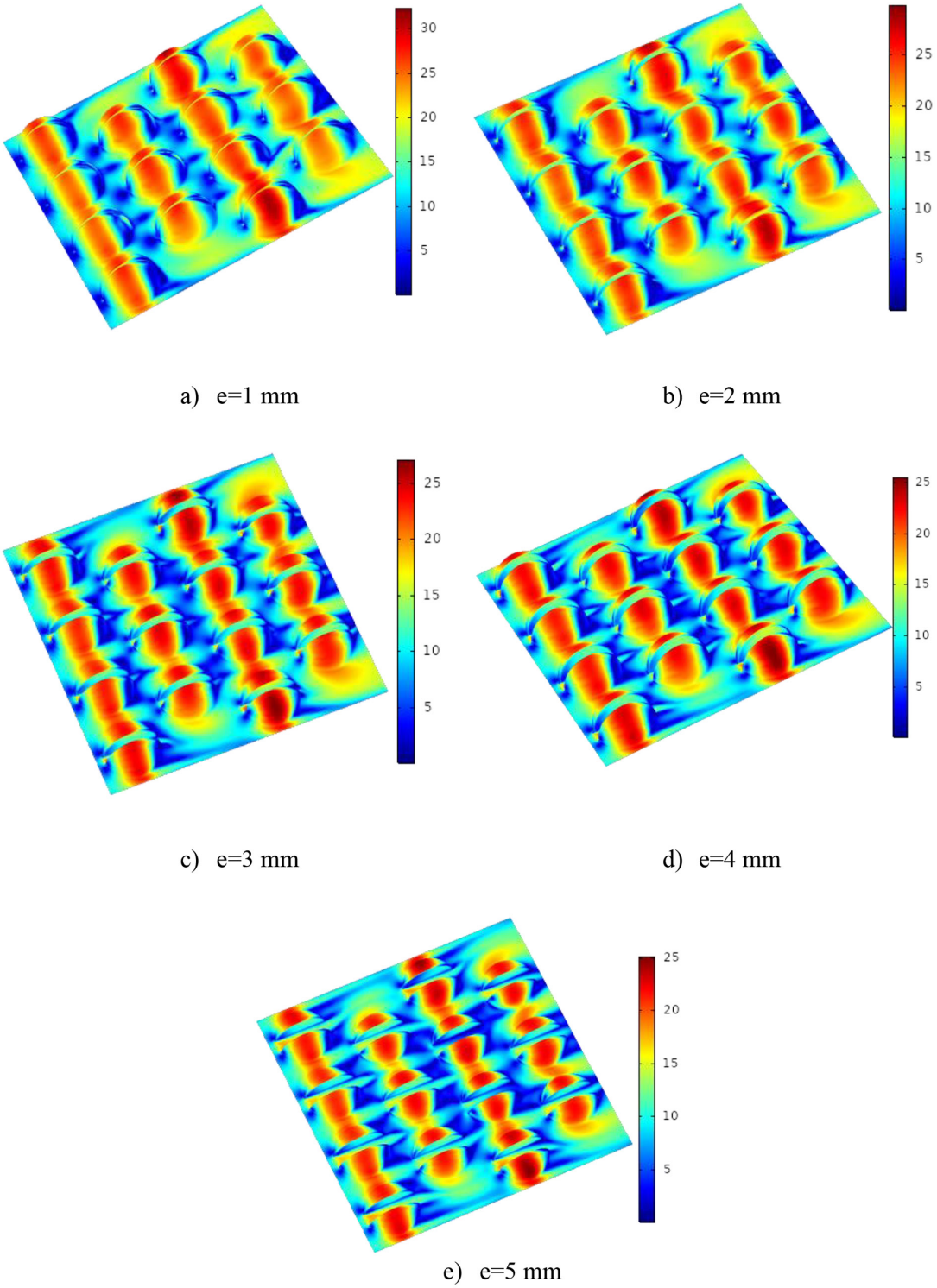

Fig. 12. Velocities on the sink surface contact for e=1, 2, 3, 4, 5 mm and *Re* = 21367

higher Re, the reduction in the Δp is about 45%. Figure 15 depicts R_{th} versus *Re* where R_{th} decline is observed by augmenting Re. This is due to incremented turbulent intensity and reduced velocity fluctuations, where, a remarkable reduction around 90% in R_{th} is obtained for the two cases at the highest Re. As a result, the outcomes of various situations are determined using identical boundary conditions. Figure 16 shows a 100% improvement in the hydrothermal performance factor (HTPF) compared to that of cylindrical pin fins heat sink. Furthermore, Figure 17 illustrates the thermal field and velocities at the vicinity of the plate. The case of three trenches is examined

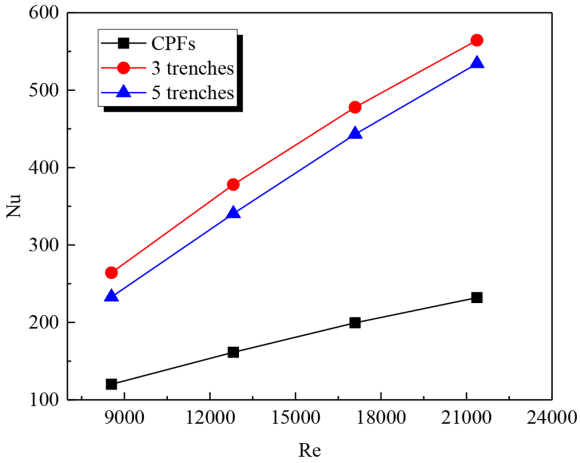

Fig. 13. Nusselt number vs *Re*, for e=1 mm

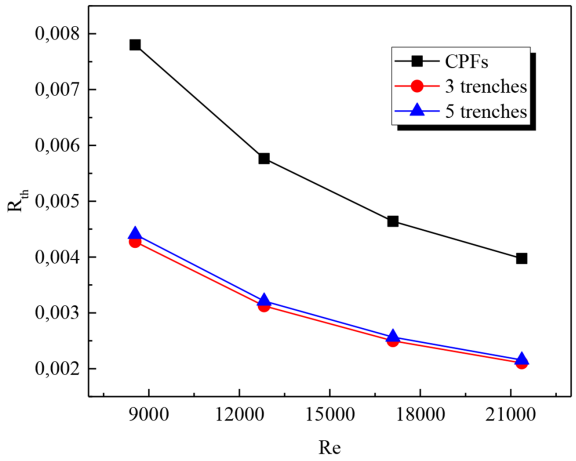

Fig. 15. Variation of the thermal resistance (R_{th}) with *Re,* for e=1 mm

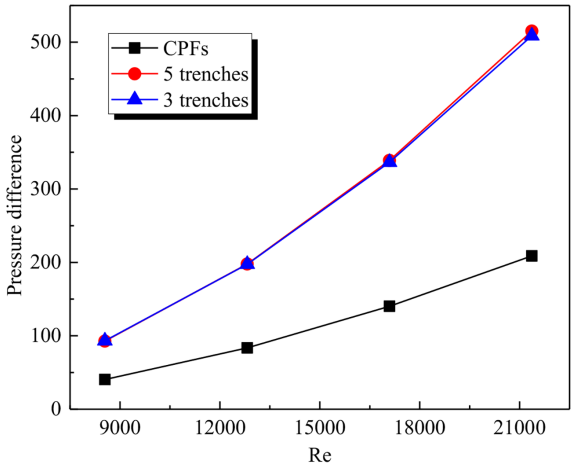

Fig. 14. Pressure difference (Δp) vs *Re*, for e=1 mm

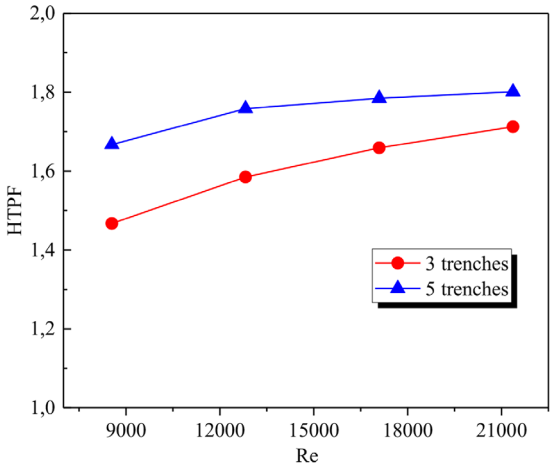

Fig. 16. Variation of the HTPF with Re, for e=1 mm

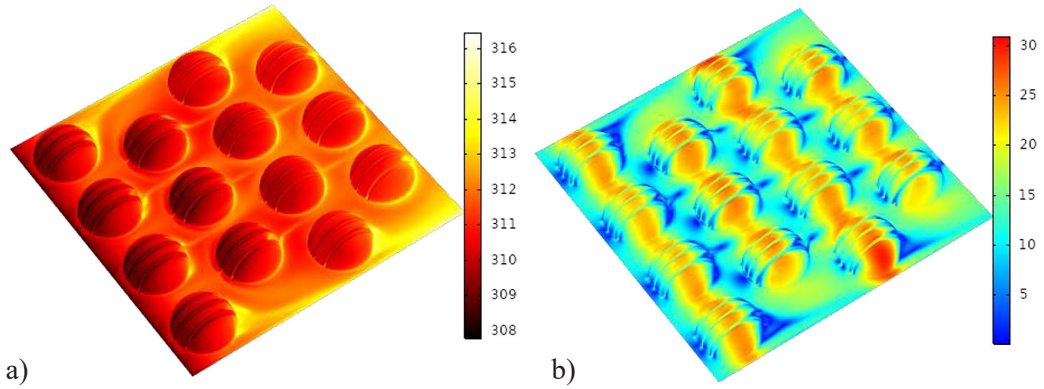

Fig. 17. Illustration of (a) the thermal and (b) hydrodynamical field for the case of three trenches at Re = 21367

at Re = 21367. Augmenting the cooling-air velocity noticeably reduces system temperatures. The design of a trenched-hemispherical heat sink has been put forward. In addition, it is evident that the outlet air temperatures are higher compared with those at the inlet. This is primarily due to the number and thickness of the trenches in the heat sink.

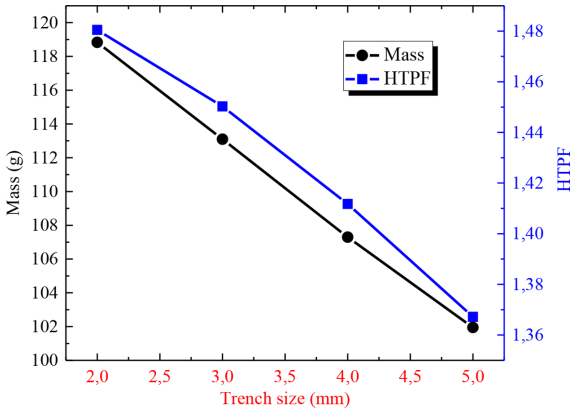

Fig. 18. Variation of the heat sink mass and HTPF with the trench size

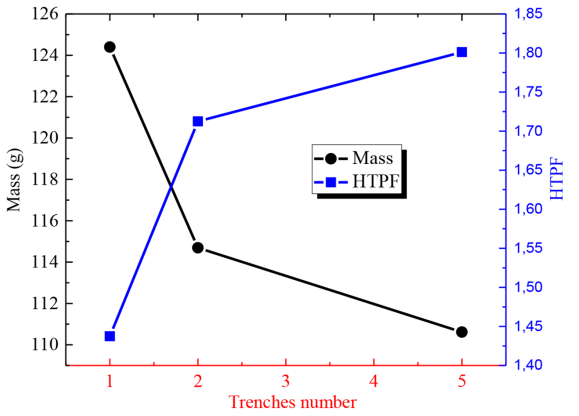

Fig. 19. Variation of the heat sink mass and HTPF with the trenches number, for e=1 mm

Mass of HSs

Enhancement of thermal performance is crucial for design of heat sinks. However, the technological quality of heat sinks is influenced by several factors, including the contact surface area, mass, as well as the occupied volume. The present work, proposes an optimization model to not only enhance the heat dissipation in heat sinks but also to effectively decrease their mass and occupied volume. The variation of heat sink mass and HTPF with the trench size (Fig. 18). Obviously, the trench size helps reduce the mass and increase the thermal and dynamic performance by 16.5% and 8.8% respectively. In this study, the new design can improve the thermal management and reduce the mass as well as downsize the system, resulting in cost reduction when compared with the classical cylindrical pin fins heat sink [30]. Figure 19 depicts variation of the heat sink mass (g) and HTPF with the trench number. Higher HTPF is shown for the case of hemispherical heat sink having five trenches, the heat sink mass decreases by 12.5%.

CONCLUSIONS

Various configurations of trenched hemispherical pin fins heat sink are numerically studied. Different trench number and thickness are investigated. Air flow behavior and heat transfer are examined for various Reynold numbers. Conclusions drawn are summarized as follows:

- hemispherical pin fins heat sink fitted with a trench in the middle considerably increases the heat transfer surface rate;

Nomenclature

$\overline{u_i' u_j'}$	Reynolds stress [m²/s²]
$\overline{u_i' \theta}$	Turbulent heat flux [m·K/s]
x	Cartesian coordinate vector [m]
v	Kinematic viscosity [m²/s]
$\overline{P}$	Modified kinematic pressure [m²/s²]
Δp	Pressure drops [Pa]
w	Specific dissipation rate [1/s]
α	Thermal diffusivity [m²/s]
k	Turbulent kinetic energy [m²/s²]
i,j	Velocity vector [m/s]
q''	Thermal diffusivity [W/m²]
μ	Dynamic viscosity [kg/(m·s)]
A	Total heat transfer surface area [m²]
c_p	Specific heat [J/(kg·K)]
d	Height of the hemi spherical pin fins [m]
D_h	Hydraulic diameter [m]
H	Height of channel inlet [m]
Nu	Nusselt number
Pr	Prandtl number
Re	Reynolds number
R_{th}	Thermal resistance [K·m²/W]
S_L/H	Pitch length ratio of pin fins
S_W/H	Pitch transverse ratio of pin fins
T	Temperature [K]
U	Mean velocity [m/s]
λ	Thermal conductivity [W/(m²·K)]
ρ	Density [kg/m³]
i, j	Tensor index
in	Inlet
out	Outlet
s	Solid
w	Wall

- trenched fins improve the thermal performance and reduce the material mass and cost;
- trenched fins reduce the fin mass by 12.5% while improving the performance by 100% compared to the non-trenched fins;
- trenches help reducing the wall temperature and augmenting the air velocity around the pin fins;
- trench thickness of e = 0.1 mm is shown to ensure the highest heat dissipation rate;
- hemispherical heat sink having a trench thickness of e = 1 mm increases the Nusselt number by 45% and decreases the thermal resistance by 42%;
- pressure drop of 50% is observed compared to the conventional heat sink configuration i.e. CPFHS.

For future research, various trench shapes could be investigated for the sake of higher cooling performance.

Acknowledgments

The authors are thankful to the Deanship of Graduate Studies and Scientific Research at University of Bisha for supporting this work through the Fast-Track Research Support Program.

REFERENCES

1. H.M. Ali, A. Arshad, Experimental investigation of n-eicosane based circular pin-fin heat sinks for passive cooling of electronic devices, International Journal of Heat and Mass Transfer, 112 (2017) 649-661.
2. K. Bilen, U. Akyol, S. Yapici, Heat transfer and friction correlations and thermal performance analysis for a finned surface, Energy Conversion and Management, 42(9) (2001) 1071-1083.
3. E.R. Meinders, T.H. Van Der Meer, K. Hanjalic, Local convective heat transfer from an array of wall-mounted cubes, International Journal of Heat and Mass Transfer, 41(2) (1998) 335-346.
4. O.N. Sara, T. Pekdemir, S. Yapici, M. Yilmaz, Heat-transfer enhancement in a channel flow with perforated rectangular blocks, International Journal of Heat and Fluid Flow, 22(5) (2001) 509-518.
5. A. Yousfi, D. Sahel, M. Mellal, Effects of A Pyramidal Pin Fins on CPU Heat Sink Performances, Journal of Advanced Research in Fluid Mechanics and Thermal Sciences, 63(2) (2020) 260-273.
6. M.R. Shaeri, M. Yaghoubi, Numerical analysis of turbulent convection heat transfer from an array of perforated fins, International Journal of Heat and Fluid Flow, 30(2) (2009) 218-228.
7. M.F. Ismail, M.N. Hasan, M. Ali, Numerical simulation of turbulent heat transfer from perforated plate-fin heat sinks, Heat and Mass Transfer, 50(4) (2014) 509-519.
8. G. Song, D.-H. Kim, D.-H. Song, J.-B. Sung, S.-J. Yook, Heat-dissipation performance of cylindrical heat sink with perforated fins, International Journal of Thermal Sciences, 170 (2021) 107132.
9. T.K. Ibrahim, A.T. Al-Sammarraie, W.H. Al-Taha, M.R. Salimpour, M. Al-Jethelah, A.N. Abdalla, H. Tao, Experimental and numerical investigation of heat transfer augmentation in heat sinks using perforation technique, Applied Thermal Engineering, 160 (2019) 113974.
10. M. Reid, C. Sun, M. El Sayed, Topology Optimization of Heat Sinks for High Efficiency Electronics Employing Simplified Convection Model, in: AIAA Scitech 2020 Forum, American Institute of Aeronautics and Astronautics, 2020.
11. C.-H. Huang, Y.-C. Liu, H. Ay, The design of optimum perforation diameters for pin fin array for heat transfer enhancement, International Journal of Heat and Mass Transfer, 84 (2015) 752-765.
12. S. Zeng, Q. Sun, P.S. Lee, Thermohydraulic analysis of a new fin pattern derived from topology optimized heat sink structures, International Journal of Heat and Mass Transfer, 147 (2020) 118909.
13. D. Sahel, L. Bellahcene, A. Yousfi, A. Subasi, Numerical investigation and optimization of a heat sink having hemispherical pin fins, International Communications in Heat and Mass Transfer, 122 (2021) 105133.
14. Y.-H. Pan, R. Zhao, Y.-L. Nian, W.-L. Cheng, Numerical study on heat transfer characteristics of a pin–fin staggered manifold microchannel heat sink, Applied Thermal Engineering, 219 (2023) 119436.
15. H. Babar, H. Wu, H.M. Ali, W. Zhang, Hydrothermal performance of inline and staggered arrangements of airfoil shaped pin-fin heat sinks: A comparative study, Thermal Science and Engineering Progress, 37 (2023) 101616.
16. M. Abuşka, V. Çorumlu, A comparative experimental thermal performance analysis of conical pin fin heat sink with staggered and modified staggered layout under forced convection, Thermal Science and Engineering Progress, 37 (2023) 101560.
17. A. Heidarshenas, Z. Azizi, S.M. Peyghambarzadeh, S. Sayyahi, Experimental investigation of heat transfer enhancement using ionic liquid-Al2O3 hybrid nanofluid in a cylindrical microchannel heat sink, Applied Thermal Engineering, 191 (2021) 116879.
18. R. Avinash Kumar, M. Kavitha, P. Manoj Kumar, S. Arvindh Seshadri, Numerical study of graphene-platinum hybrid nanofluid in microchannel for

electronics cooling, Proceedings of the Institution of Mechanical Engineers, Part C: Journal of Mechanical Engineering Science, 235(21) (2021) 5845-5857.

19. G. Sriharan, S. Harikrishnan, H.M. Ali, Enhanced heat transfer characteristics of the mini hexagonal tube heat sink using hybrid nanofluids, Nanotechnology, 33(47) (2022) 475403.
20. D. Yang, Y. Wang, G. Ding, Z. Jin, J. Zhao, G. Wang, Numerical and experimental analysis of cooling performance of single-phase array microchannel heat sinks with different pin-fin configurations, Applied Thermal Engineering, 112 (2017) 1547-1556.
21. K.-S. Yang, W.-H. Chu, I.-Y. Chen, C.-C. Wang, A comparative study of the airside performance of heat sinks having pin fin configurations, International Journal of Heat and Mass Transfer, 50(23) (2007) 4661-4667.
22. Y. Khetib, K. Sedraoui, A. Gari, Numerical study of the effects of pin geometry and configuration in micro-pin-fin heat sinks for turbulent flows, Case Studies in Thermal Engineering, 27 (2021) 101243.
23. K. Nilpueng, M. Mesgarpour, L.G. Asirvatham, A.S. Dalkılıç, H.S. Ahn, O. Mahian, S. Wongwises, Effect of pin fin configuration on thermal performance of plate pin fin heat sinks, Case Studies in Thermal Engineering, 27 (2021) 101269.
24. K. Yakut, N. Alemdaroglu, I. Kotcioglu, C. Celik, Experimental investigation of thermal resistance of a heat sink with hexagonal fins, Applied Thermal Engineering, 26(17) (2006) 2262-2271.
25. R. Pakrouh, M.J. Hosseini, A.A. Ranjbar, R. Bahrampoury, A numerical method for PCM-based pin fin heat sinks optimization, Energy Conversion and Management, 103 (2015) 542-552.
26. R. Baby, C. Balaji, Thermal optimization of PCM based pin fin heat sinks: An experimental study, Applied Thermal Engineering, 54(1) (2013) 65-77.
27. M. Sivashankar, C. Selvam, Experimental investigation on the thermal performance of low-concentrated photovoltaic module using various pin-fin configurations of heat sink with phase change materials, Journal of Energy Storage, 55 (2022) 105575.
28. A. Arshad, H.M. Ali, M. Ali, S. Manzoor, Thermal performance of phase change material (PCM) based pin-finned heat sinks for electronics devices: Effect of pin thickness and PCM volume fraction, Applied Thermal Engineering, 112 (2017) 143-155.
29. H.M. Ali, M.J. Ashraf, A. Giovannelli, M. Irfan, T.B. Irshad, H.M. Hamid, F. Hassan, A. Arshad, Thermal management of electronics: An experimental analysis of triangular, rectangular and circular pin-fin heat sinks for various PCMs, International Journal of Heat and Mass Transfer, 123 (2018) 272-284.
30. S.-B. Chin, J.-J. Foo, Y.-L. Lai, T.K.-K. Yong, Forced convective heat transfer enhancement with perforated pin fins, Heat and Mass Transfer, 49(10) (2013) 1447-1458.
31. Y.-T. Yang, H.-S. Peng, Investigation of planted pin fins for heat transfer enhancement in plate fin heat sink, Microelectronics Reliability, 49(2) (2009) 163-169.
32. C. Multiphysics, CFD Module User 's Guide, COMSOL Multiphysics ed., 2016.